

Magnetoelastic effects in multiferroic fibrous composite with imperfect interface

X. Wang and E. Pan

Department of Civil Engineering and Department of Applied Mathematics, University of Akron, Akron, Ohio 44325-3905, USA
(Received 29 August 2007; published 13 December 2007)

This paper investigates the magnetoelastic responses of multiferroic fibrous composites with imperfectly bonded interface under longitudinal shear. The proposed imperfect interface model is a natural generalization of the shear lag (or the spring layer) model. By virtue of the complex variable method, we first consider the case where an isolated circular multiferroic fiber is imperfectly bonded to an infinite multiferroic matrix. Very concise expressions for the complex field potentials characterizing the magnetoelastic fields inside and outside the circular fiber are obtained when the matrix is subjected to the remote uniform magnetoelastic loading. The Mori-Tanaka mean-field method is then employed to derive the effective moduli of the multiferroic fibrous composite made of randomly distributed fibers reinforced to the matrix. Particularly we demonstrate that the interfacial imperfection in elasticity, electricity, and magnetism will always cause a significant reduction in the magnetoelastic coefficient of the BaTiO₃-CoFe₂O₄ fibrous composite.

DOI: 10.1103/PhysRevB.76.214107

PACS number(s): 81.05.Ni, 75.80.+q, 77.65.-j

I. INTRODUCTION

The magnetoelastic (ME) effect, which is defined as the induction of an electric polarization by a magnetic field or the induction of a magnetization by an electric field in multiferroic composites composed of ferroelectric and ferromagnetic phases, is a focus research topic, both theoretically¹⁻¹⁰ and experimentally.¹¹⁻¹³ The multiferroic composite can be laminated composite (2-2 connectivity),¹⁻⁶ fibrous composite (1-3 or 3-1 connectivity),⁷⁻¹⁰ or composite with 0-3 or 3-0 connectivity,¹ or 2-1 connectivity.¹² A comprehensive review of recent research activities on the linear ME effect was presented by Fiebig.¹⁴ Generally speaking the ME effect in the multiferroic composite is achieved through the product property: a magnetic field applied to the multiferroic composite will induce strain in the ferromagnetic phase which is passed through the interface to the ferroelectric phase, where it induces an electric polarization.^{7,14} Therefore the interface is critical in achieving the ME effect. In earlier investigation the interface between the ferroelectric and ferromagnetic constituents was primarily assumed to be perfect or ideal coupling,^{1,2,6-10} resulting in large deviations between theory and experiment. An improvement was made by Bichurin *et al.*⁴ who introduced an interface coupling parameter k that defines the degree to which the deformation of the piezoelectric layer follows that of the magnetostrictive layer. Nan *et al.*³ studied the influence of the interfacial bonding on the ME effect in the multiferroic laminated composite of Terfenol-D and PZT by means of the Green's function technique. It is noted that these structure models are confined to the multiferroic laminated composite.^{3,4} To the best of the authors' knowledge, however, the influence of the imperfectly bonded interface on the ME effect in multiferroic fibrous composite has not been investigated thoroughly.

This investigation is, therefore, concerned with the ME effect in multiferroic fibrous composite with imperfect interface under longitudinal shear. Both the fiber and matrix are assumed to be transversely isotropic (6 mm material symmetry about the fiber axis). The imperfect interface proposed is a natural extension of the shear lag model (or the spring layer

model).¹⁵⁻²¹ (i) tractions are continuous but displacements are discontinuous across the imperfect interface. The jumps in displacement components are further assumed to be proportional, in terms of the "spring-factor-type" interface parameters, to their respective interface traction components; (ii) the normal electric displacement is continuous but the electric potential is discontinuous across the interface. The jump in the electric potential is proportional to the normal electric displacement; (iii) the normal magnetic flux is continuous but the magnetic potential is discontinuous across the interface. The jump in the magnetic potential is proportional to the normal magnetic flux. This general imperfect interface, which could model various interfacial damages (e.g., debonding, sliding and/or cracking across the interface) and could also simulate the thin glue layer between any two adjacent phases, is termed the mechanically compliant, dielectrically and magnetically weakly conducting interface.²⁰

This paper is organized as follows. In Sec. II, by means of the complex variable method, an analytical solution is obtained for an isolated circular cylindrical multiferroic fiber embedded in an infinite multiferroic matrix.^{16,20} The Mori-Tanaka mean-field approximation^{9,10,22-26} is then adopted in Sec. III to analyze the overall magnetoelastic behaviors of the multiferroic composite with finite fiber concentrations. In Sec. IV, as an important application, we discuss the ME effect of the BaTiO₃-CoFe₂O₄ multiferroic fibrous composite with imperfectly bonded interface. Conclusions are drawn in Sec. V.

II. AN ISOLATED MULTIFERROIC FIBER

A. Basic formulation

Consider first an isolated multiferroic fiber with a circular cross section (phase 2) of radius R embedded in an infinite multiferroic matrix (phase 1), as shown in Fig. 1. Both the fiber and matrix are 6 mm material symmetry about the fiber axis. At infinity, the matrix is subjected to the anti-plane shear stresses $\sigma_{zx}^\infty, \sigma_{zy}^\infty$, and the in-plane electric displacements D_x^∞, D_y^∞ and magnetic fluxes B_x^∞, B_y^∞ . Thus the two-

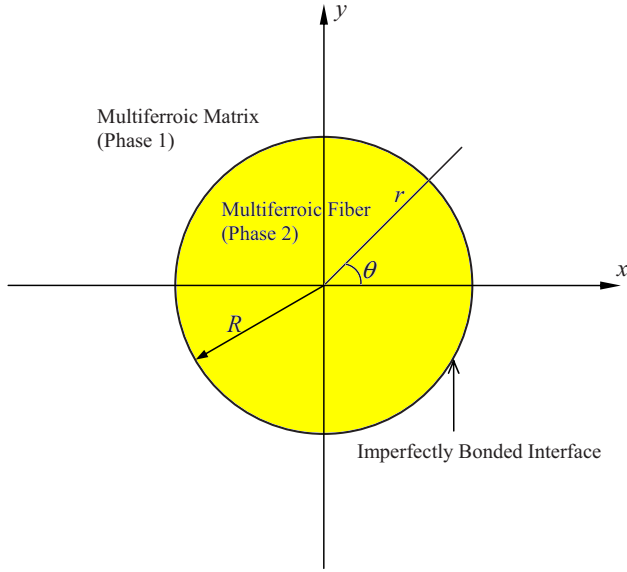


FIG. 1. (Color online) A multiferroic circular cylindrical fiber of radius R imperfectly bonded to an infinite multiferroic matrix. The polarization and magnetization directions are along the fiber axis.

phase composite system is in a state of anti-plane deformation described by

$$\begin{aligned} u_x = u_y = 0, \quad u_z = w(x, y), \\ \phi = \phi(x, y), \quad \varphi = \varphi(x, y), \end{aligned} \quad (1)$$

where u_x , u_y , u_z , denote the displacement components in the x , y , and z directions, respectively; ϕ and φ are the electric and magnetic potentials.

The constitutive equations become

$$\begin{aligned} \sigma_{zx} &= c_{44} \frac{\partial w}{\partial x} + e_{15} \frac{\partial \phi}{\partial x} + q_{15} \frac{\partial \varphi}{\partial x}, \\ D_x &= e_{15} \frac{\partial w}{\partial x} - \varepsilon_{11} \frac{\partial \phi}{\partial x} - \alpha_{11} \frac{\partial \varphi}{\partial x}, \\ B_x &= q_{15} \frac{\partial w}{\partial x} - \alpha_{11} \frac{\partial \phi}{\partial x} - \mu_{11} \frac{\partial \varphi}{\partial x}, \end{aligned} \quad (2a)$$

$$\begin{aligned} \sigma_{zy} &= c_{44} \frac{\partial w}{\partial y} + e_{15} \frac{\partial \phi}{\partial y} + q_{15} \frac{\partial \varphi}{\partial y}, \\ D_y &= e_{15} \frac{\partial w}{\partial y} - \varepsilon_{11} \frac{\partial \phi}{\partial y} - \alpha_{11} \frac{\partial \varphi}{\partial y}, \\ B_y &= q_{15} \frac{\partial w}{\partial y} - \alpha_{11} \frac{\partial \phi}{\partial y} - \mu_{11} \frac{\partial \varphi}{\partial y}, \end{aligned} \quad (2b)$$

where σ_{kz} , D_k , B_k , ($k=x, y$), c_{44} , e_{15} , q_{15} , ε_{11} , α_{11} , μ_{11} are the stresses, electric displacements, magnetic fluxes, elastic modulus, piezoelectric coefficient, piezomagnetic coefficient, dielectric permittivity, ME coefficient, and the magnetic permeability, respectively.

Under this antiplane deformation, the governing equations are simplified to

$$\begin{aligned} c_{44} \nabla^2 w + e_{15} \nabla^2 \phi + q_{15} \nabla^2 \varphi &= 0, \\ e_{15} \nabla^2 w - \varepsilon_{11} \nabla^2 \phi - \alpha_{11} \nabla^2 \varphi &= 0, \\ q_{15} \nabla^2 w - \alpha_{11} \nabla^2 \phi - \mu_{11} \nabla^2 \varphi &= 0, \end{aligned} \quad (3)$$

where $\nabla^2 = \frac{\partial^2}{\partial x^2} + \frac{\partial^2}{\partial y^2}$ is the two-dimensional Laplace operator.

Next we introduce the generalized displacement vector $\mathbf{U} = [w \ \phi \ \varphi]^T$ and the generalized stress function vector Φ , which is related to the stresses, electric displacements, and magnetic fluxes through the following relations:

$$\begin{bmatrix} \sigma_{zy} \\ D_y \\ B_y \end{bmatrix} = \Phi_{,x}, \quad \begin{bmatrix} \sigma_{zx} \\ D_x \\ B_x \end{bmatrix} = -\Phi_{,y}. \quad (4)$$

In addition we define the generalized stiffness matrix \mathbf{L} as

$$\mathbf{L} = \begin{bmatrix} c_{44} & e_{15} & q_{15} \\ e_{15} & -\varepsilon_{11} & -\alpha_{11} \\ q_{15} & -\alpha_{11} & -\mu_{11} \end{bmatrix}, \quad (5)$$

which is real and symmetric but not positive definite.

It can be shown that the generalized displacement and stress function vectors can be concisely expressed in terms of an analytic function vector $\mathbf{f}(z)$ of a single complex variable $z = x + iy = r \exp(i\theta)$ as²⁰

$$\mathbf{U} = \text{Im}\{\mathbf{f}(z)\}, \quad \Phi = \mathbf{L} \text{Re}\{\mathbf{f}(z)\}. \quad (6)$$

Furthermore, the strains, stresses, electric fields, electric displacements, magnetic fields, and magnetic fluxes can also be concisely expressed in terms of $\mathbf{f}(z)$ as follows:

$$\begin{bmatrix} \gamma_{zy} + i\gamma_{zx} \\ -E_y - iE_x \\ -H_y - iH_x \end{bmatrix} = \mathbf{f}'(z), \quad \begin{bmatrix} \sigma_{zy} + i\sigma_{zx} \\ D_y + iD_x \\ B_y + iB_x \end{bmatrix} = \mathbf{L}'\mathbf{f}'(z), \quad (7)$$

where the strains γ_{zx} and γ_{zy} , the electric fields E_x and E_y , the magnetic fields H_x and H_y are related to w , ϕ , and φ through

$$\begin{aligned} \gamma_{zx} &= w_{,x}, \quad \gamma_{zy} = w_{,y}, \\ E_x &= -\phi_{,x}, \quad E_y = -\phi_{,y}, \\ H_x &= -\varphi_{,x}, \quad H_y = -\varphi_{,y}. \end{aligned} \quad (8)$$

B. The generalized shear lag model for the imperfect fiber-matrix interface

In order to model various possible damages occurring on the fiber-matrix interface and to simulate the thin glue layer existing between two adjacent phases, we adopt the following generalized shear lag model,¹⁵⁻²¹ which can be teamed as the mechanically compliant, dielectrically and magnetically weakly conducting interface:²¹

$$\sigma_{zr}^{(1)} = \sigma_{zr}^{(2)}, \quad w^{(1)} - w^{(2)} = \alpha \sigma_{zr}^{(2)},$$

$$D_r^{(1)} = D_r^{(2)}, \quad \phi^{(1)} - \phi^{(2)} = -\beta D_r^{(2)},$$

$$B_r^{(1)} = B_r^{(2)}, \quad \varphi^{(1)} - \varphi^{(2)} = -\gamma B_r^{(2)}, \quad \text{on } r = R, \quad (9)$$

where α , β , and γ are three non-negative parameters. It is noted that $\alpha = \beta = \gamma = 0$ corresponds to a perfect interface studied previously,⁸⁻¹⁰ whereas $\alpha, \beta, \gamma \rightarrow \infty$ describes a completely debonded and charge-free interface.

C. The field potentials

The imperfect interface conditions in Eq. (9) can also be expressed in terms of two analytic function vectors $\mathbf{f}_1(z)$ defined in the matrix and $\mathbf{f}_2(z)$ defined in the fiber, as follows:

$$\begin{aligned} \mathbf{L}_2 \mathbf{f}_2^+(z) + \mathbf{L}_2 \bar{\mathbf{f}}_2^-\left(\frac{R^2}{z}\right) &= \mathbf{L}_1 \mathbf{f}_1^+(z) + \mathbf{L}_1 \bar{\mathbf{f}}_1^-\left(\frac{R^2}{z}\right), \\ \mathbf{f}_1^+(z) - \bar{\mathbf{f}}_1^-\left(\frac{R^2}{z}\right) - \mathbf{f}_2^+(z) + \bar{\mathbf{f}}_2^-\left(\frac{R^2}{z}\right) \\ &= \Lambda \mathbf{L}_2 \left[z \mathbf{f}_2^+(z) - \frac{R^2}{z} \bar{\mathbf{f}}_2^-\left(\frac{R^2}{z}\right) \right] \quad (|z| = R), \end{aligned} \quad (10)$$

where

$$\Lambda = \frac{1}{R} \begin{bmatrix} \alpha & 0 & 0 \\ 0 & -\beta & 0 \\ 0 & 0 & -\gamma \end{bmatrix}. \quad (11)$$

It follows from Eq. (10) that

$$\begin{aligned} \mathbf{f}_1(z) &= \mathbf{L}_1^{-1} \mathbf{L}_2 \bar{\mathbf{f}}_2^-\left(\frac{R^2}{z}\right) + \mathbf{L}_1^{-1} \mathbf{k} z - \mathbf{L}_1^{-1} \bar{\mathbf{k}} R^2 z^{-1}, \\ \bar{\mathbf{f}}_1\left(\frac{R^2}{z}\right) &= \mathbf{L}_1^{-1} \mathbf{L}_2 \mathbf{f}_2(z) - \mathbf{L}_1^{-1} \mathbf{k} z + \mathbf{L}_1^{-1} \bar{\mathbf{k}} R^2 z^{-1}, \end{aligned} \quad (12)$$

where the vector \mathbf{k} is related to the remote loading as

$$\mathbf{k} = \begin{bmatrix} \sigma_{zy}^\infty + i\sigma_{zx}^\infty \\ D_y^\infty + iD_x^\infty \\ B_y^\infty + iB_x^\infty \end{bmatrix}. \quad (13)$$

Substituting Eq. (12) into Eq. (10) and eliminating $\bar{\mathbf{f}}_1^-(z)$ and $\bar{\mathbf{f}}_1^+\left(\frac{R^2}{z}\right)$, we finally arrive at

$$\begin{aligned} (\mathbf{I} + \mathbf{L}_1^{-1} \mathbf{L}_2) \bar{\mathbf{f}}_2^-\left(\frac{R^2}{z}\right) + \Lambda \mathbf{L}_2 \frac{R^2}{z} \bar{\mathbf{f}}_2^-\left(\frac{R^2}{z}\right) - 2\mathbf{L}_1^{-1} \bar{\mathbf{k}} R^2 z^{-1} \\ = (\mathbf{I} + \mathbf{L}_1^{-1} \mathbf{L}_2) \mathbf{f}_2^+(z) + \Lambda \mathbf{L}_2 z \mathbf{f}_2^+(z) - 2\mathbf{L}_1^{-1} \mathbf{k} z \quad (|z| = R). \end{aligned} \quad (14)$$

Apparently the left-hand side of the above expression is analytic outside the fiber including the point at infinity, whilst the right-hand side of the above expression is analytic within the fiber. Consequently we arrive at the following set of differential equations:

$$(\mathbf{I} + \mathbf{L}_1^{-1} \mathbf{L}_2) \mathbf{f}_2(z) + \Lambda \mathbf{L}_2 z \mathbf{f}_2'(z) = 2\mathbf{L}_1^{-1} \mathbf{k} z \quad (|z| < R) \quad (15)$$

with its solution expediently given by

$$\mathbf{f}_2(z) = 2\mathbf{L}_2^{-1} (\mathbf{L}_1^{-1} + \mathbf{L}_2^{-1} + \Lambda)^{-1} \mathbf{L}_1^{-1} \mathbf{k} z \quad (|z| < R). \quad (16)$$

In view of Eqs. (12) and (16), the expression of $\mathbf{f}_1(z)$ is then given by

$$\mathbf{f}_1(z) = [2\mathbf{L}_1^{-1} (\mathbf{L}_1^{-1} + \mathbf{L}_2^{-1} + \Lambda)^{-1} - \mathbf{I}] \mathbf{L}_1^{-1} \bar{\mathbf{k}} R^2 z^{-1} + \mathbf{L}_1^{-1} \mathbf{k} z \quad (|z| > R).$$

Once the two analytic function vectors $\mathbf{f}_1(z)$ and $\mathbf{f}_2(z)$ are known, it is easy to obtain the magneto-electroelastic field in and outside the circular cylindrical fiber by using Eqs. (6) and (7). For example, it is easy to find that the mechanical strains, the electric and magnetic fields are all uniform inside the circular fiber with their values being given by

$$\begin{bmatrix} \gamma_{zy} + i\gamma_{zx} \\ -E_y - iE_x \\ -H_y - iH_x \end{bmatrix} = 2\mathbf{L}_2^{-1} (\mathbf{L}_1^{-1} + \mathbf{L}_2^{-1} + \Lambda)^{-1} \mathbf{L}_1^{-1} \mathbf{k}, \quad r < R. \quad (18)$$

However, outside the fiber, i.e., in the matrix, they are space dependent and distributed as

$$\begin{bmatrix} \gamma_{zy} + i\gamma_{zx} \\ -E_y - iE_x \\ -H_y - iH_x \end{bmatrix} = \mathbf{L}_1^{-1} \mathbf{k} - \left(\frac{R}{r}\right)^2 \exp(-2i\theta) [2\mathbf{L}_1^{-1} \times (\mathbf{L}_1^{-1} + \mathbf{L}_2^{-1} + \Lambda)^{-1} - \mathbf{I}] \mathbf{L}_1^{-1} \bar{\mathbf{k}}, \quad r > R. \quad (19)$$

The results obtained in this section will be employed in the following section to obtain the overall magneto-electroelastic behaviors of multiferroic composites with finite inclusion concentration.

III. THE EFFECTIVE MODULI

We assume that the aligned circular multiferroic fibers of same radius are randomly distributed on the x - y plane and that all the imperfect circular fiber-matrix interfaces are identical (i.e., the matrix Λ is the same for all the interfaces), then the fiber-reinforced multiferroic composite is also transversely isotropic with the x - y plane being the isotropic plane. By employing the Mori-Tanaka mean-field method,^{9,10,22-27} the effective moduli of the multiferroic fibrous composite with the imperfectly bonded interface can be derived as

$$\begin{aligned} \mathbf{L}_c = \mathbf{L}_1 [(1 + c_2) \mathbf{L}_1 - 2c_2 (\mathbf{L}_1^{-1} + \mathbf{L}_2^{-1} + \Lambda)^{-1}]^{-1} [(1 - c_2) \mathbf{L}_1 \\ + 2c_2 (\mathbf{L}_1^{-1} + \mathbf{L}_2^{-1} + \Lambda)^{-1}], \end{aligned} \quad (20)$$

where c_2 is the volume fraction of the multiferroic fibers. Apparently the symmetric condition $\mathbf{L}_c = \mathbf{L}_c^T$ is satisfied. In Eq. (20) the effective moduli \mathbf{L}_c are defined as

$$\begin{bmatrix} \langle \sigma_{zy} \rangle \\ \langle D_y \rangle \\ \langle B_y \rangle \end{bmatrix} = \mathbf{L}_c \begin{bmatrix} \langle \gamma_{zy} \rangle \\ \langle -E_y \rangle \\ \langle -H_y \rangle \end{bmatrix}, \quad \begin{bmatrix} \langle \sigma_{zx} \rangle \\ \langle D_x \rangle \\ \langle B_x \rangle \end{bmatrix} = \mathbf{L}_c \begin{bmatrix} \langle \gamma_{zx} \rangle \\ \langle -E_x \rangle \\ \langle -H_x \rangle \end{bmatrix}, \quad (21)$$

where $\langle \cdots \rangle$ stands for the average value. A detailed derivation of Eq. (20) is given in the Appendix.

It is obvious that if the interface is perfect, i.e., $\Lambda=0$, then Eq. (20) reduces to

$$\begin{aligned} \mathbf{L}_c &= \mathbf{L}_1[(1+c_2)\mathbf{L}_1 - 2c_2(\mathbf{L}_1^{-1} + \mathbf{L}_2^{-1})^{-1}][(1-c_2)\mathbf{L}_1 \\ &\quad + 2c_2(\mathbf{L}_1^{-1} + \mathbf{L}_2^{-1})^{-1}] \\ &= \mathbf{L}_1[(1+c_2)\mathbf{L}_1 + (1-c_2)\mathbf{L}_2]^{-1}[(1-c_2)\mathbf{L}_1 + (1+c_2)\mathbf{L}_2] \\ &= \mathbf{L}_1[(1+c_2)\mathbf{L}_1 + c_1\mathbf{L}_2]^{-1}[c_1\mathbf{L}_1 + (1+c_2)\mathbf{L}_2], \end{aligned} \quad (22)$$

where $c_1=1-c_2$ is the volume fraction of the multiferroic matrix. Equation (22) is just the expression of the effective moduli of the multiferroic composite with perfect interface in the framework of composite cylinder assemblage (CCA) derived by Benveniste.⁸ Therefore, it is of interest to notice that the present prediction of Mori-Tanaka scheme coincides with the CCA result. We further point out that Benveniste²⁵ also derived the effective thermal conductivity of the composite with spherical particles in the presence of thermal contact resistance at interphase boundaries by using the generalized self-consistent scheme and the Mori-Tanaka theory, and thus Eq. (20) for the case of fibrous system and the coupled field with imperfect interfaces derived in this article can be considered as the counterpart of Eq. (14) in Ref. 25. We finally observe from Eq. (20) that the effective moduli for the imperfect interface case are equivalent to those of a virtual composite, where the circular fibers with the virtual moduli $\hat{\mathbf{L}}_2=(\mathbf{L}_2^{-1}+\Lambda)^{-1}$ are perfectly bonded to the matrix.

IV. APPLICATION: THE ME EFFECT OF BaTiO₃-COFe₂O₄ FIBROUS COMPOSITE

In Sec. III we have obtained in Eq. (20) the effective moduli \mathbf{L}_c of the multiferroic fibrous composite with imperfectly bonded interface. Equation (20) demonstrates the presence of the ME coefficient α_{11} for the composite with piezoelectric fibers reinforced in magnetostrictive matrix or conversely magnetostrictive fibers reinforced in piezoelectric matrix (It is noted that in either piezoelectric or magnetostrictive phase, there is no ME effect). To show the influence of the imperfect interface on the ME effect more clearly, we consider two typical cases: (i) a composite consisting of the magnetostrictive CoFe₂O₄ matrix reinforced by the piezoelectric BaTiO₃ fibers and (ii) a composite consisting of the piezoelectric BaTiO₃ matrix reinforced by the magnetostrictive CoFe₂O₄ fibers. The pertinent material properties of BaTiO₃ are $c_{44}=43 \times 10^9$ N/m², $e_{15}=11.6$ C/m², $\epsilon_{11}=11.2 \times 10^{-9}$ C²/N m², $\mu_{11}=5 \times 10^{-6}$ N s²/C²; while those of CoFe₂O₄ are $c_{44}=45.3 \times 10^9$ N/m², $q_{15}=550$ m/A, $\epsilon_{11}=0.08 \times 10^{-9}$ C²/N m², $\mu_{11}=590 \times 10^{-6}$ N s²/C².

A. A composite consisting of CoFe₂O₄ matrix reinforced by BaTiO₃ fibers

Figure 2 shows the ME coefficient α_{11} as a function of the BaTiO₃ volume fraction c_2 and for different interfacial im-

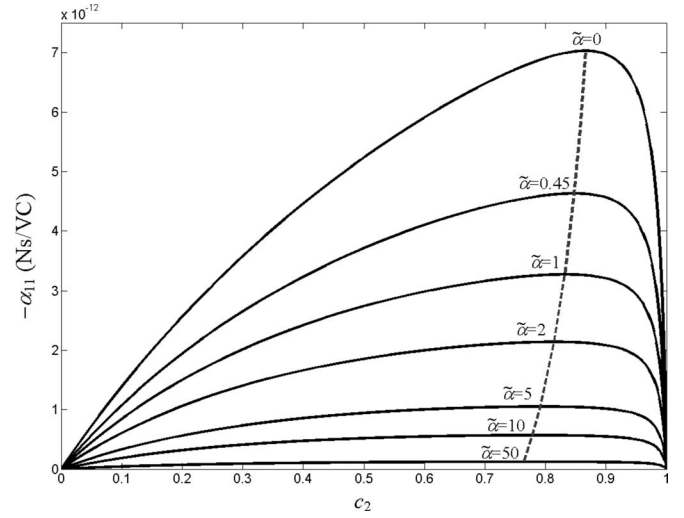


FIG. 2. Variation of the ME coefficient α_{11} vs. volume fraction c_2 of BaTiO₃ for different interfacial imperfections in elasticity characterized by $\alpha=\tilde{\alpha}R/c_{44}^{(2)}$ and $\beta=\gamma=0$ with $\tilde{\alpha}$ being a dimensionless parameter. CoFe₂O₄ matrix reinforced by BaTiO₃ fiber.

perfections (only in elasticity) characterized by $\alpha=\tilde{\alpha}R/c_{44}^{(2)}$ and $\beta=\gamma=0$ with $\tilde{\alpha}$ being a dimensionless parameter. It is found that the ME coefficient decreases as $\tilde{\alpha}$ increases (i.e., the interface becomes more compliant), a phenomenon similar to that observed in multiferroic laminated composites.³ Furthermore the optimal value of the BaTiO₃ volume fraction, at which the maximum ME coefficient occurs, decreases as the interface becomes more compliant. Figures 3 and 4 show the ME coefficient α_{11} as a function of the BaTiO₃ volume fraction c_2 : (1) for the interfacial imperfection (in dielectricity) characterized by $\beta=\tilde{\beta}R/\epsilon_{11}^{(2)}$ and $\alpha=\gamma=0$ with $\tilde{\beta}$ being a dimensionless parameter (Fig. 3) and (2) for the interfacial imperfection (in magnetism) characterized by $\gamma=\tilde{\gamma}R/\mu_{11}^{(2)}$ and $\alpha=\beta=0$ with $\tilde{\gamma}$ being a dimensionless

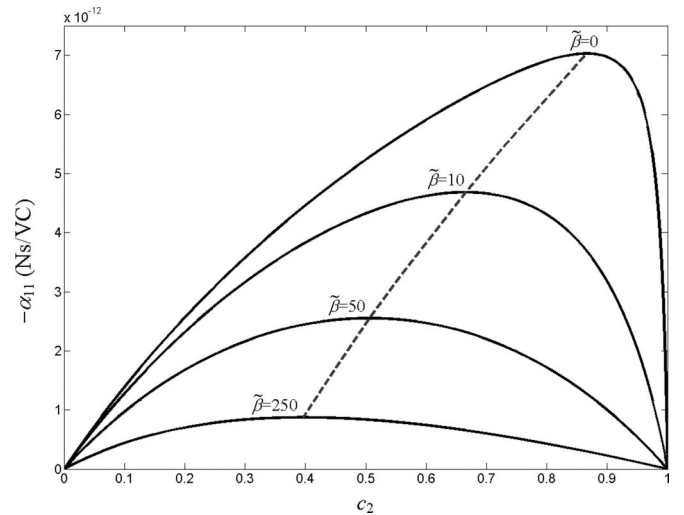


FIG. 3. Variation of the ME coefficient α_{11} vs. volume fraction c_2 of BaTiO₃ for different interfacial imperfections in dielectricity characterized by $\beta=\tilde{\beta}R/\epsilon_{11}^{(2)}$ and $\alpha=\gamma=0$ with $\tilde{\beta}$ being a dimensionless parameter. CoFe₂O₄ matrix reinforced by BaTiO₃ fiber.

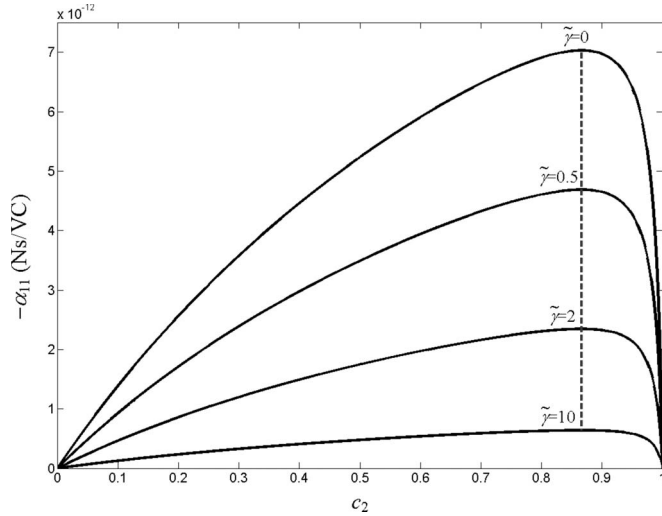


FIG. 4. Variation of the ME coefficient α_{11} vs. volume fraction c_2 of BaTiO₃ for different interfacial imperfections in magnetism characterized by $\gamma = \tilde{\gamma}R/\mu_{11}^{(2)}$ and $\alpha = \beta = 0$ with $\tilde{\gamma}$ being a dimensionless parameter. CoFe₂O₄ matrix reinforced by BaTiO₃ fiber.

parameter (Fig. 4). It is observed from Figs. 3 and 4 that the ME coefficient decreases as $\tilde{\beta}$ or $\tilde{\gamma}$ increases. In addition the optimal value of the BaTiO₃ volume fraction, at which the maximum ME coefficient occurs, decreases significantly as $\tilde{\beta}$ increases (Fig. 3); while its optimal fraction value basically remains the same as $\tilde{\gamma}$ increases (Fig. 4).

B. A composite consisting of BaTiO₃ matrix reinforced by CoFe₂O₄ fibers

Figure 5 shows the ME coefficient α_{11} as a function of the CoFe₂O₄ volume fraction c_2 and for the interfacial imperfection (only in elasticity) characterized by $\alpha = \tilde{\alpha}R/c_{44}^{(2)}$ and $\beta = \gamma = 0$. Similarly, Figs. 6 and 7 illustrate α_{11} as a function of

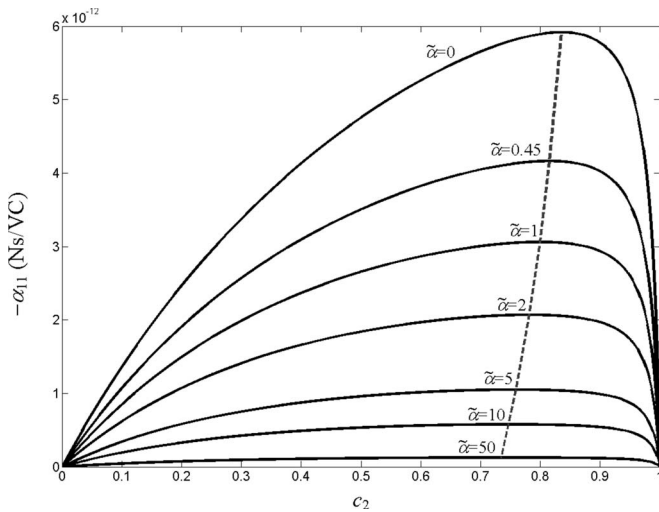


FIG. 5. Variation of the ME coefficient α_{11} vs. volume fraction c_2 of CoFe₂O₄ for different interfacial imperfections in elasticity characterized by $\alpha = \tilde{\alpha}R/c_{44}^{(2)}$ and $\beta = \gamma = 0$ with $\tilde{\alpha}$ being a dimensionless parameter. BaTiO₃ matrix reinforced by CoFe₂O₄ fiber.

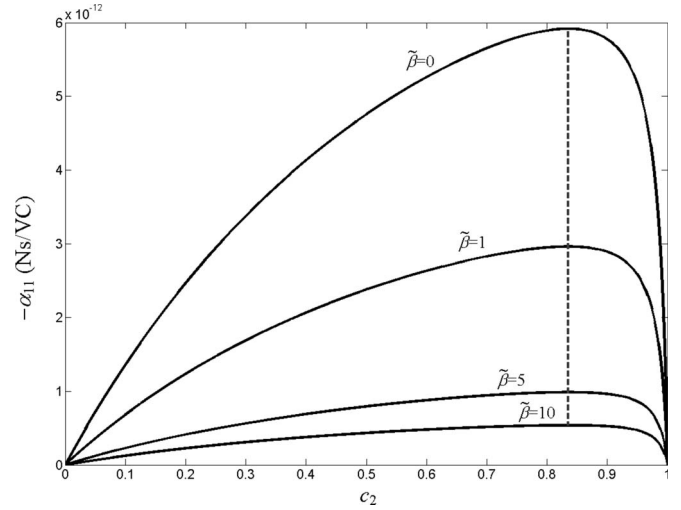


FIG. 6. Variation of the ME coefficient α_{11} vs. volume fraction c_2 of CoFe₂O₄ for different interfacial imperfections in dielectricity characterized by $\beta = \tilde{\beta}R/\epsilon_{11}^{(2)}$ and $\alpha = \gamma = 0$ with $\tilde{\beta}$ being a dimensionless parameter. BaTiO₃ matrix reinforced by CoFe₂O₄ fiber.

the CoFe₂O₄ volume fraction c_2 : (1) for the interfacial imperfection (in dielectricity) characterized by $\beta = \tilde{\beta}R/\epsilon_{11}^{(2)}$ and $\alpha = \gamma = 0$ (Fig. 6) and (2) for the interfacial imperfection (in magnetism) characterized by $\gamma = \tilde{\gamma}R/\mu_{11}^{(2)}$ and $\alpha = \beta = 0$ (Fig. 7). It is observed that when the interface is perfect ($\alpha = \beta = \gamma = 0$), the maximum ME coefficient ($|\alpha_{11}| = 5.92 \times 10^{-12}$ N s/VC when $c_2 = 0.835$) for a composite consisting of BaTiO₃ matrix reinforced by CoFe₂O₄ fibers is smaller than that ($|\alpha_{11}| = 7.03 \times 10^{-12}$ N s/VC when $c_2 = 0.866$) for a composite consisting of CoFe₂O₄ matrix reinforced by BaTiO₃ fibers. Similar to the previous case, the imperfection in elasticity, dielectricity and magnetism will always cause a reduction in the ME effect. Different to the previous case, however, the optimal value of the CoFe₂O₄ volume fraction,

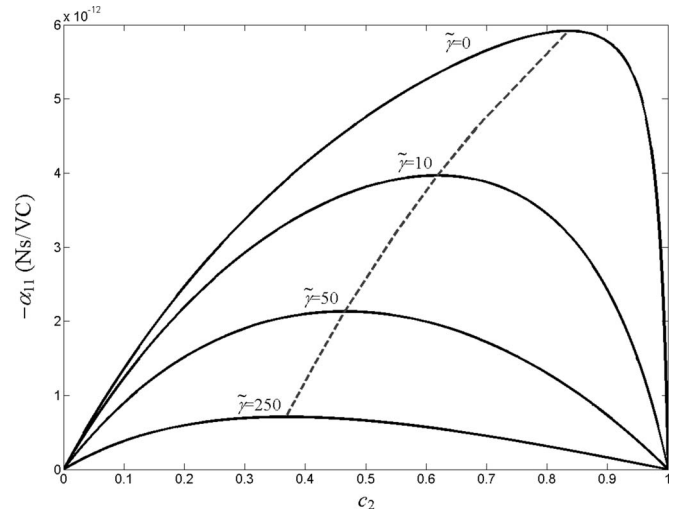


FIG. 7. Variation of the ME coefficient α_{11} vs. volume fraction c_2 of CoFe₂O₄ for different interfacial imperfections in magnetism characterized by $\gamma = \tilde{\gamma}R/\mu_{11}^{(2)}$ and $\alpha = \beta = 0$ with $\tilde{\gamma}$ being a dimensionless parameter. BaTiO₃ matrix reinforced by CoFe₂O₄ fiber.

at which the maximum ME effect occurs, decreases significantly as $\tilde{\gamma}$ increases (Fig. 7), whilst its value basically remains the same as $\tilde{\beta}$ increases (Fig. 6).

V. CONCLUSIONS

A theoretical model incorporating the interfacial imperfection has been established for studying the ME effect in multiferroic fibrous composites. The generalized shear lag model for the imperfect interface is introduced in Eq. (9) to account for possible interfacial damage and to simulate the thin glue layer between the two phases. A compact matrix expression for the effective moduli of the multiferroic fibrous composite with imperfect interface is obtained (Eq. (20)). Numerical results demonstrate that the interfacial imperfection in elasticity, electricity and magnetism will all cause a significant reduction in the (ME) effect. Therefore, the influence of the interfacial imperfection on the ME effect is important and cannot be ignored in general.

ACKNOWLEDGMENTS

This work was supported in part by AFRL/ARL.

APPENDIX: A DETAILED DERIVATION OF Eq. (20)

In order to describe the overall behavior of the multiferroic composite, we focus on a representative volume element (RVE). In addition we assume that the RVE is subjected to the loadings σ_{zy}^∞ , D_y^∞ , and B_y^∞ . The volume-averaged values within the RVE can be proved to be²⁵⁻²⁷

$$\begin{aligned} \begin{bmatrix} \langle \sigma_{zy} \rangle \\ \langle D_y \rangle \\ \langle B_y \rangle \end{bmatrix} &= (1 - c_2) \begin{bmatrix} \langle \sigma_{zy} \rangle_1 \\ \langle D_y \rangle_1 \\ \langle B_y \rangle_1 \end{bmatrix} + c_2 \begin{bmatrix} \langle \sigma_{zy} \rangle_2 \\ \langle D_y \rangle_2 \\ \langle B_y \rangle_2 \end{bmatrix}, \\ \begin{bmatrix} \langle \gamma_{zy} \rangle \\ \langle -E_y \rangle \\ \langle -H_y \rangle \end{bmatrix} &= (1 - c_2) \begin{bmatrix} \langle \gamma_{zy} \rangle_1 \\ \langle -E_y \rangle_1 \\ \langle -H_y \rangle_1 \end{bmatrix} + c_2 \begin{bmatrix} \langle \gamma_{zy} \rangle_2 \\ \langle -E_y \rangle_2 \\ \langle -H_y \rangle_2 \end{bmatrix} \\ &+ \frac{c_2}{\pi R^2} \oint_l \begin{bmatrix} (w^{(1)} - w^{(2)}) \\ (\phi^{(1)} - \phi^{(2)}) \\ (\varphi^{(1)} - \varphi^{(2)}) \end{bmatrix} \hat{n}_2 dl, \end{aligned} \quad (\text{A1})$$

where $\langle \cdots \rangle_1$ and $\langle \cdots \rangle_2$ refer to the averages over volumes of the matrix and fiber respectively, the line integral is taken along the perimeter l of a typical fiber and \hat{n}_2 the y component of the unit normal vector on the interface in the outward direction with respect to the fiber. In addition $\langle \sigma_{zy} \rangle = \sigma_{zy}^\infty$, $\langle D_y \rangle = D_y^\infty$, $\langle B_y \rangle = B_y^\infty$.

By employing the results of Eq. (18) in Sec. II, it is found that

$$\begin{bmatrix} \langle \sigma_{zy} \rangle_2 \\ \langle D_y \rangle_2 \\ \langle B_y \rangle_2 \end{bmatrix} = 2(\mathbf{L}_1^{-1} + \mathbf{L}_2^{-1} + \Lambda)^{-1} \mathbf{L}_1^{-1} \begin{bmatrix} \langle \sigma_{zy} \rangle_1 \\ \langle D_y \rangle_1 \\ \langle B_y \rangle_1 \end{bmatrix}. \quad (\text{A2})$$

Substituting the above into Eq. (A1), we obtain

$$\begin{bmatrix} \langle \sigma_{zy} \rangle_1 \\ \langle D_y \rangle_1 \\ \langle B_y \rangle_1 \end{bmatrix} = [2c_2(\mathbf{L}_1^{-1} + \mathbf{L}_2^{-1} + \Lambda)^{-1} \mathbf{L}_1^{-1} + (1 - c_2)\mathbf{I}]^{-1} \begin{bmatrix} \sigma_{zy}^\infty \\ D_y^\infty \\ B_y^\infty \end{bmatrix}. \quad (\text{A3})$$

In addition we have

$$\begin{aligned} \begin{bmatrix} \langle \gamma_{zy} \rangle_1 \\ \langle -E_y \rangle_1 \\ \langle -H_y \rangle_1 \end{bmatrix} &= \mathbf{L}_1^{-1} \begin{bmatrix} \langle \sigma_{zy} \rangle_1 \\ \langle D_y \rangle_1 \\ \langle B_y \rangle_1 \end{bmatrix}, \\ \begin{bmatrix} \langle \gamma_{zy} \rangle_2 \\ \langle -E_y \rangle_2 \\ \langle -H_y \rangle_2 \end{bmatrix} &= \mathbf{L}_2^{-1} \begin{bmatrix} \langle \sigma_{zy} \rangle_2 \\ \langle D_y \rangle_2 \\ \langle B_y \rangle_2 \end{bmatrix}, \end{aligned} \quad (\text{A4})$$

$$\frac{1}{\pi R^2} \oint_l \begin{bmatrix} (w^{(1)} - w^{(2)}) \\ (\phi^{(1)} - \phi^{(2)}) \\ (\varphi^{(1)} - \varphi^{(2)}) \end{bmatrix} \hat{n}_2 dl = \Lambda \begin{bmatrix} \langle \sigma_{zy} \rangle_2 \\ \langle D_y \rangle_2 \\ \langle B_y \rangle_2 \end{bmatrix}.$$

In view of Eqs. (A3) and (A4), Eq. (A1) can be finally expressed as

$$\begin{aligned} \begin{bmatrix} \langle \gamma_{zy} \rangle \\ \langle -E_y \rangle \\ \langle -H_y \rangle \end{bmatrix} &= \mathbf{L}_1^{-1} [(1 + c_2)\mathbf{L}_1 \\ &- 2c_2(\mathbf{L}_1^{-1} + \mathbf{L}_2^{-1} + \Lambda)^{-1}] [(1 - c_2)\mathbf{L}_1 \\ &+ 2c_2(\mathbf{L}_1^{-1} + \mathbf{L}_2^{-1} + \Lambda)^{-1}]^{-1} \begin{bmatrix} \sigma_{zy}^\infty \\ D_y^\infty \\ B_y^\infty \end{bmatrix}. \end{aligned} \quad (\text{A5})$$

Comparison of Eq. (A5) with Eq. (21) will immediately lead to the effective moduli as

$$\begin{aligned} \mathbf{L}_c &= \mathbf{L}_c^T \\ &= [(1 - c_2)\mathbf{L}_1 + 2c_2(\mathbf{L}_1^{-1} + \mathbf{L}_2^{-1} + \Lambda)^{-1}] [(1 + c_2)\mathbf{L}_1 \\ &- 2c_2(\mathbf{L}_1^{-1} + \mathbf{L}_2^{-1} + \Lambda)^{-1}]^{-1} \mathbf{L}_1 = \mathbf{L}_1 [(1 + c_2)\mathbf{L}_1 - 2c_2(\mathbf{L}_1^{-1} \\ &+ \mathbf{L}_2^{-1} + \Lambda)^{-1}]^{-1} [(1 - c_2)\mathbf{L}_1 + 2c_2(\mathbf{L}_1^{-1} + \mathbf{L}_2^{-1} + \Lambda)^{-1}]. \end{aligned} \quad (\text{A6})$$

- ¹G. Harshé, Ph.D. thesis, Pennsylvania State University, State College, 1991.
- ²G. Harshé, J. P. Dougherty, and R. E. Newnham, *Int. J. Appl. Electromagn. Mater.* **4**, 145 (1993); M. Avellaneda and G. Harshé, *J. Intell. Mater. Syst. Struct.* **5**, 501 (1994).
- ³C. W. Nan, G. Liu, and Y. H. Lin, *Appl. Phys. Lett.* **83**, 4366 (2003).
- ⁴M. I. Bichurin, V. M. Petrov, and G. Srinivasan, *Phys. Rev. B* **68**, 054402 (2003); V. M. Petrov, G. Srinivasan, M. I. Bichurin and A. Gupta, *ibid.* **75**, 224407 (2007).
- ⁵S. X. Dong, J. F. Li, and D. Viehland, *IEEE Trans. Ultrason. Ferroelectr. Freq. Control* **50**, 1253 (2003); S. X. Dong, J. F. Li, and D. Viehland, *J. Mater. Sci.* **41**, 97 (2006).
- ⁶Z. Huang, *J. Appl. Phys.* **100**, 114104 (2006).
- ⁷C. W. Nan, *Phys. Rev. B* **50**, 6082 (1994).
- ⁸Y. Benveniste, *Phys. Rev. B* **51**, 16424 (1995).
- ⁹J. H. Huang and W. S. Kuo, *J. Appl. Phys.* **81**, 1378 (1997).
- ¹⁰J. Y. Li and M. L. Dunn, *J. Intell. Mater. Syst. Struct.* **9**, 404 (1998).
- ¹¹H. Zheng, J. Wang, S. E. Lofland, Z. Ma, L. Mohaddes-Ardabili, T. Zhao, L. Salamanca-Riba, S. R. Shinde, S. B. Ogale, F. Bai, D. Viehland, Y. Jia, D. G. Schlom, M. Wuttig, A. Roytburd, and R. Ramesh, *Science* **303**, 661 (2004).
- ¹²S. X. Dong, J. Y. Zhai, J. F. Li, and D. Viehland, *Appl. Phys. Lett.* **89**, 243512 (2006); **89**, 252904 (2006).
- ¹³Y. H. Chu, T. Zhao, M. P. Cruz, Q. Zhan, P. L. Yang, L. W. Martin, M. Huijben, C. H. Yang, F. Zavaliche, H. Zheng, and R. Ramesh, *Appl. Phys. Lett.* **90**, 252906 (2007).
- ¹⁴M. Fiebig, *J. Phys. D* **38**, R123 (2005).
- ¹⁵Y. Benveniste and T. Miloh, *Int. J. Eng. Sci.* **24**, 1537 (1986).
- ¹⁶C. Q. Ru and P. Schiavone, *Proc. R. Soc. London, Ser. A* **453**, 2551 (1997).
- ¹⁷Y. Benveniste, *J. Appl. Phys.* **86**, 1273 (1999); Y. Benveniste, *J. Phys. Chem. Solids* **54**, 708 (2006).
- ¹⁸T. Chen, *Int. J. Solids Struct.* **38**, 3081 (2001).
- ¹⁹H. Fan and K. Y. Sze, *Mech. Mater.* **33**, 363 (2001); H. Fan and G. F. Wang, *ibid.* **35**, 943 (2003); H. Fan, J. S. Yang, and L. M. Xu, *Appl. Phys. Lett.* **88**, 203509 (2006).
- ²⁰X. Wang and E. Pan, *Phys. Status Solidi B* **224**, 1940 (2007); X. Wang, E. Pan, and A. K. Roy, *J. Mech. Phys. Solids* (to be published); X. Wang and E. Pan, *Open Mech. J.* **1**, 1 (2007).
- ²¹H. M. Shodja, S. M. Tabatabaei, and M. T. Kamali, *Int. J. Solids Struct.* **44**, 6361 (2007).
- ²²T. Mori and K. Tanaka, *Acta Metall.* **21**, 571 (1973).
- ²³G. J. Weng, *Int. J. Eng. Sci.* **22**, 845 (1984).
- ²⁴Y. Benveniste, *Mech. Mater.* **6**, 147 (1987).
- ²⁵Y. Benveniste, *J. Appl. Phys.* **61**, 2840 (1987).
- ²⁶L. H. He and C. W. Lim, *Compos. Sci. Technol.* **61**, 579 (2001).
- ²⁷L. H. He and C. W. Lim, *Composites, Part B* **34**, 373 (2003).